STUDIA UBB. CHEMIA, LV, 3, 2010

CHARACTERIZATION OF SOME SnO_2 CERAMICS WITH ZnO AND Sb_2O_3 ADDITIVES

MARIA GOREA[a], RODICA CREȚ[b], DELIA MARIA SIMUȚ[a]

ABSTRACT. The paper concerns obtaining SnO_2 ceramics with addition of 1, respectively 2 % mol ZnO, and of 0.01 %, 0.05 % and respectively 0.1 % mol Sb_2O_3. The oxides were mixed in wet state, in ethanol. The thermal treatment was experimented at three temperatures (1150, 1200 and 1250 ˚C) defined based on the results of the dilatometric analysis. Apparent density, compactness and electrical characteristics of ceramics depend on both sintering temperature, and the dopant type and amount. By doping, ceramics with about 85 % of the theoretic density were obtained. Electrical resistivity increases with the amount of dopant.

Keywords: *ceramics, tin dioxide, dopant*

INTRODUCTION

Tin dioxide, SnO_2, represents an n-type semiconductor with a rutile-type crystalline structure. Semiconductors may be used for detecting gases such as H_2, CO, hydrocarbons, other gases and organic vapours. They have become part of modern life, ceramic sensors being preferred due to their chemical and physical stability in aggressive environments, to their easy-processing, and to the possibility of achieving pre-defined properties in their case. The n-type semiconductor sensors are based on the superficial adsorption of oxygen leading to an increase of electrical resistance, which then decreases if a reducing gas reacts with the adsorbed oxygen. A lot of oxides (SnO_2, ZnO, TiO_2, ZrO_2) have been studied as materials for obtaining sensitive ceramics, however this research involving the identification of new methods and materials is still on top as consequence of the need of solving specific requirements – such as sensibility, selectivity, feedback time, density, and less but not least, the fabrication costs [1-5]. SnO_2-based ceramics are used for the fabrication of gas sensors, but their disadvantage is a low density (about 50 % from the theoretical one). The level of densification for such ceramics can be improved by adding dopants like CoO, MnO, ZnO, CuO or Bi_2O_3. By adding 0.5-1 % mol of dopant, the ceramics' density may increase

[a] *Babeş-Bolyai University, Faculty of Chemistry and Chemical Engineering, 11 Arany Janos Str., RO-400084, Cluj-Napoca, Romania, mgorea@chem.ubbcluj.ro*
[b] *Technical University, Faculty of Electrical Engineering, 26-28 G. Bariţiu Str. RO-400027, Cluj-Napoca, Romania, rodica_cret@yahoo.fr*

up to 95 % from the theoretical one [6-9]. Doping with an oxide of divalent and one of a pentavalent metal may lead to densification of ceramics and in the same time to its varistor-type electrical behaviour (nonlinear pattern of resistivity). Oxide systems based on SnO_2 and ZnO were intensely studied as both gas sensors, and varistors [10,11]. Under normal circumstances, this leads first to an increase of the resistance of the circuit, then to its decrease due to the reaction of the reducing gas with the adsorbed oxygen [12-13]. In the case of dense ceramics with SnO_2, the role of ZnO used as dopant is to realize oxygen vacancies, *i.e.* Zn''_{Sn}+ V^{**}_o type defects that lead to the formation of Schottky barriers and finally, to the densification of the material [14]. Doping is also an effective mean for controlling the crystallites size. By using dopants such as Pd, Pt, Sb_2O_3, or MgO, the sensibility and sensitivity of the sensor can be highly improved [15, 16].

This paper concerns SnO_2-containing ceramics with addition of ZnO and Sb_2O_3 from the point of view of sintering temperatures, compactness characteristics and correlation with electrical properties.

RESULTS AND DISCUSSION

Tin dioxide (SnO_2) represents an n-type semiconductor with a rutile-type crystalline structure; after sintering the powders, the final ceramic products show low densities. The high diffusion coefficient of oxygen even at low temperatures, and the stability of Sn^{2+} oxidation state may promote loss of oxygen and vacancies creation. Also, during the thermal treatment, in the presence of dopants, substitutions occur in the crystalline network of SnO_2, influencing the electrical properties of ceramics, and densification of the material.

$$SnO_2(s) \xrightarrow{1200\ ^\circ C} SnO(g) + \tfrac{1}{2}\, O_2$$
$$ZnO \rightarrow Zn''_{Sn} + V_0^{**} + O_0^{x}$$
$$Sb_2O_3 \rightarrow 2Sb'_{Sn} + V_0^{**} + 3/2\, O_2$$

The influence of ZnO and Sb_2O_3 on the sintering process has been investigated by using dilatometric analysis. By observing the dilatometric results on samples with ZnO *vs.* those with both ZnO and Sb_2O_3 in a ratio of 0.1 % mol (table 5), one can notice that an increase of ZnO content from 1 to 2 % mol leads to an increase of the maximum sintering temperature from 1178.5 ˚C to 1203.9 ˚C, while the addition of Sb_2O_3 does not significantly influence the results. Thus, three sintering temperatures for the mixtures have been chosen, as follows: 1150 ˚C (samples M_1, M_2, M_5 and M_6), 1200 ˚C (samples M_1-M_8) and 1250 ˚C (samples M_3, M_4, M_7 and M_8). In the case of all compositions, an incipient sintering was noticed around 900 ˚C.

Table 1. Compactness characteristics of the studied ceramics

Sample no.	$T_{sintering}$ (˚C)	Apparent density (g/cm^3)	Relative density (% of $d_{theoretic}$)	Water adsorption (%)	Apparent porosity (%)	Firing shrinkage (%)
M_1	1150	5.429	78.115	6.439	34.879	3.555
M_2		4.457	64.129	7.344	32.716	2.557
M_5		4.398	63.281	7.213	31.675	2.644
M_6		3.845	55.320	6.901	27.233	3.029
M_1	1200	4.610	66.331	6.425	29.604	4.098
M_2		4.608	66.330	7.296	29.997	3.415
M_3		5.269	75.813	3.759	19.741	8.546
M_4		5.274	75.885	3.763	19.846	7.618
M_5		4.484	64.518	6.752	30.257	3.415
M_6		4.426	63.683	7.129	25.686	3.660
M_7		4.799	69.050	5.678	27.26	5.236
M_8		4.727	68.014	5.565	26.292	5.832
M_3	1250	5.779	83.150	1.627	9.380	10.595
M_4		5.615	80.790	2.392	13.424	9.772
M_7		4.864	69.986	4.944	23.971	6.848
M_8		5.594	80.489	4.434	24.222	7.496

Taking into account that the sensors' mechanism is mainly associated with adsorption-desorption processes, the specific surface of ceramics becomes an important factor that defines its sensitivity. Porosity may improve specific surface, so that the porous ceramics are suitable materials when it comes to sensors.

The compactness characteristics of the experimental compositions are presented in table 1.

When examining the analytical data, it can be noticed that apparent density and compactness are higher in the case of samples M_3 and M_4 fired at 1200 ˚C (about 76 % of the theoretic density and an apparent porosity of 20 %), and respectively at 1250 ˚C (more than 80 % of the theoretic density and 10 % apparent porosity). A high porosity was noticed in samples M_1 and M_2 fired at 1150 ˚C.

The current density– electric field intensity characteristics were plotted at logaritmic scale – log J = f(log E) – by measuring the intensity of the electrical field crossing the sample at a specific value of the applied voltage. These characteristics, according to the content of ZnO and Sb_2O_3 in samples fired at different temperatures are presented in figure 1a, b, c and d, while the ceramics' resistivities (calculated based on the values for the voltage, current intensity and geometrical features of the samples) are indicated in tables 2 and 3.

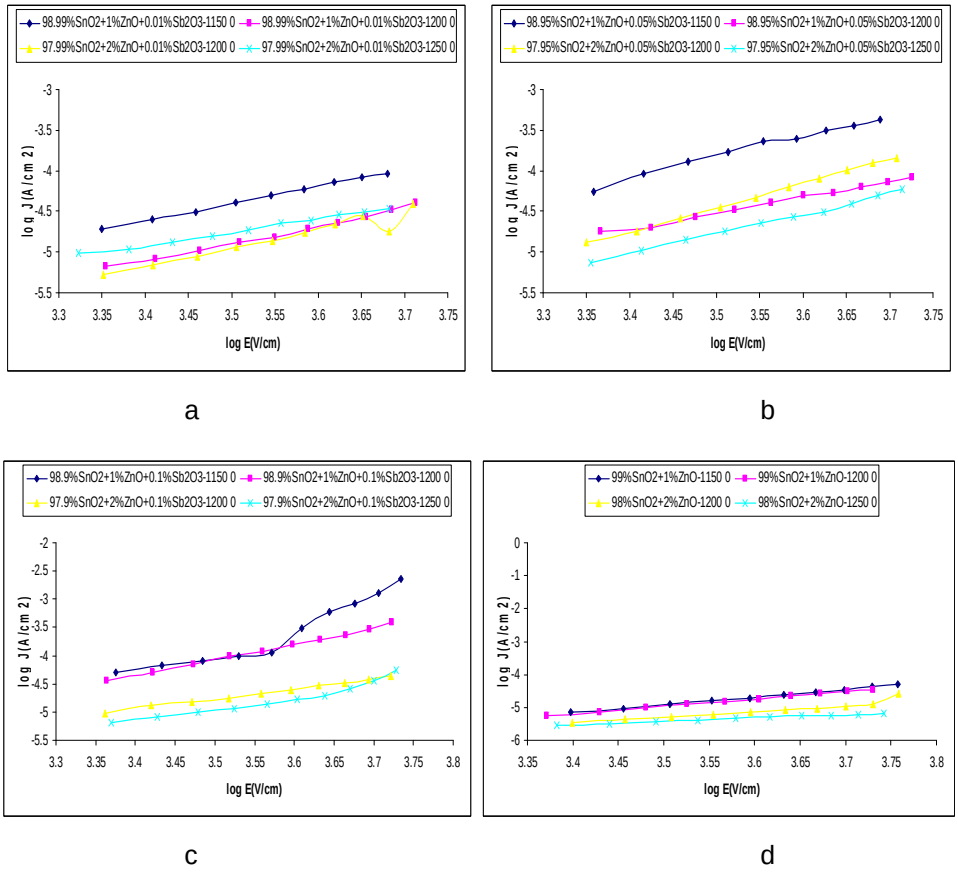

Figure 1. Current density with respect to the applied electrical field for different ZnO and Sb_2O_3 concentrations

It can be noticed that an amount of 1% mol ZnO does not influence the values of the electrical field in the case of the samples fired at 1150 ˚C and 1200 ˚C, while 2 % mol ZnO in samples fired at 1200 ˚C and 1250 ˚C slightly modifies them (figure 1 d). Significant changes of the electrical characteristics were noticed in samples doped with 1 % mol ZnO, and 0.01 respectively 0.05 % mol Sb_2O_3 fired at 1150 ˚C and 1200 ˚C; in the case of samples containing 2 % mol ZnO fired at 1200 ˚C and 1250 ˚C, the variation is minimal (figures 1 a, b). With the increase of Sb_2O_3 content to 0.1 % mol, the values of the electrical characteristics are grouped in the case of samples with 1 and respectively 2 % mol ZnO, while those with 2 % mol ZnO show higher values for the electrical resistances.

Table 2. Electrical resistivity for samples fired at 1150 ˚C and 1250 ˚C

No.	U(V)	Resistivity (MΩ·m)							
		Samples fired at 1150 ˚C				Samples fired at 1250 ˚C			
		M1	M2	M5	M6	M3	M4	M7	M8
1	700	3.4524	0.4814	0.4131	1.1719	8.5148	3.6173	3.0726	2.1949
2	900	2.5172	0.3714	0.2295	0.9216	8.3110	3.0492	2.0819	2.0131
3	1200	1.8351	0.1325	0.1601	0.6507	8.2356	2.3481	1.4302	1.5803
4	1500	1.2799	0.0395	0.1127	0.5157	8.3724	1.4044	0.9675	1,4525

Table 3. Electrical resistivity for samples fired at 1200 ˚C

No.	U(V)	Resistivity (MΩ·m)							
		Samples fired at 1200 ˚C							
		M1	M2	M3	M4	M5	M6	M7	M8
1	700	4.1499	0.6354	7.0817	2.3869	1.2964	3.3600	1.6884	4.1984
2	900	3.1171	0.4152	6.4929	1.9180	1.1147	2.7428	1.1073	3.2452
3	1200	2.2140	0.2553	5.2968	1.6088	0.8061	2.0389	0.6127	2.2162
4	1500	1.5751	0.1686	4.2834	1.2847	0.6755	1.4769	0.3819	2.6725

The electrical resistivity increases with firing temperature. The densest samples, M3 and M4, show the highest values for resistivity.

CONCLUSIONS

The sintering temperatures and the linear shrinkages of ceramic samples in the SnO_2 – ZnO – Sb_2O_3 system can be established by performing dilatometric analysis. The addition of Sb_2O_3 to SnO_2 ceramics with 1 and respectively 2 % mol ZnO influences densification and values of electrical resistivity. Electrical characteristics depend on the dopant concentration and on sintering temperature, the amount of Sb_2O_3 playing the leading role. Doping resulted in ceramics with densities up to 85 % from the theoretical density and in an increase of the electrical resistivity.

EXPERIMENTAL SECTION

In the view of obtaining the ceramics, oxides (SnO_2, Sb_2O_3 and ZnO) with high analytical purity (over 99.5 %) were used, because impurities can alter the microstructure, thus implicitly the properties – mainly the electric ones - of the final product. For a suitable processing of the mixtures, the particle size is an important factor, due to the fact that the dopants diffusion and the sintering take place in solid state, at high temperatures. The oxide particles used in these experiments have to be micrometric in size. The molar composition of the investigated system is presented in table 4.

Table 4. Experimental compositions

Composition no.	Oxide (% mol)		
	SnO_2	ZnO	Sb_2O_3
M_1	99.00	1	-
M_2	98.90	1	0.10
M_3	98.00	2	-
M_4	97.90	2	0.10
M_5	98.95	1	0.05
M_6	98.99	1	0.01
M_7	97.95	2	0.05
M_8	97.99	2	0.01

For the experiments, the proper ratios of raw materials were homogenised by using a laboratory ball mill in ethanol for 2 h. Then the samples were dried in an oven at 105 ˚C for 48 h. The powders were submitted to grain size analysis by using a Counter Coulter WING-SALD 7101 equipment. The particles for the tested compositions ranged between 0.35–6 microns in size, having an average particle size of about 2 microns.

Afterwards, the powders have been granulated and pressed as pellets by using an uniaxial press under a pressure of 800 kgf/cm^2. The dried samples have been sintered at different temperatures by the means of a laboratory furnace, the sintering temperatures being established based on dilatometric measurements. The starting and maximum sintering temperatures, as well as the linear shrinkages in the case of compositions M_1-M_4 are presented in table 5. The dilatometric analysis has been achieved on a Linseis L 75HX1400 unit, up to a maximum temperature of 1300 ˚C, with a heating rate of 10 ˚C/min, in normal atmosphere. The linear shrinkages for raw mixtures with various concentrations of dopants are presented in figure 2.

Table 5. Starting (T_{is}) and maximum (T_{max}) sintering temperatures for the studied samples

Composition (%mol)	T_{is} (˚C)	Linear shrinkage (%)	T_{max} (˚C)	Linear shrinkage (%)
M_1. 99 %SnO_2+1% ZnO	912.8	0.54	1178.5	2.39
M_2. 98.9 %SnO_2+1% ZnO+0.1% Sb_2O_3	922.1	0.57	1177.3	1.66
M_3. 98 % SnO_2+2% ZnO	907.2	0.54	1203.9	3.14
M_4. 97.9 %SnO_2+2% ZnO+0.1% Sb_2O_3	878.9	0.52	1190.1	2.51

The thermal treatment was performed in a Nabertherm laboratory-type furnace for 9 h and with 30 minutes dwell at maximum temperature; the cooling was slow, provided by the furnace's ventilation system.

The compactness characteristics of the thermally-treated samples were investigated by using the Archimedes method.

In the view of the electrical characteristics measurements (current intensity – voltage, I-V), the samples have been metallised, by covering with an Ag paste on their surface.

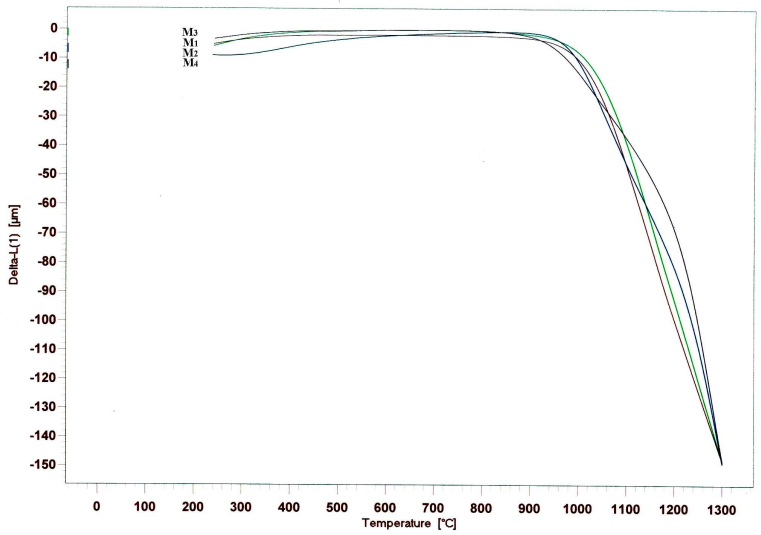

Figure 2. Linear shrinkage of the investigated samples

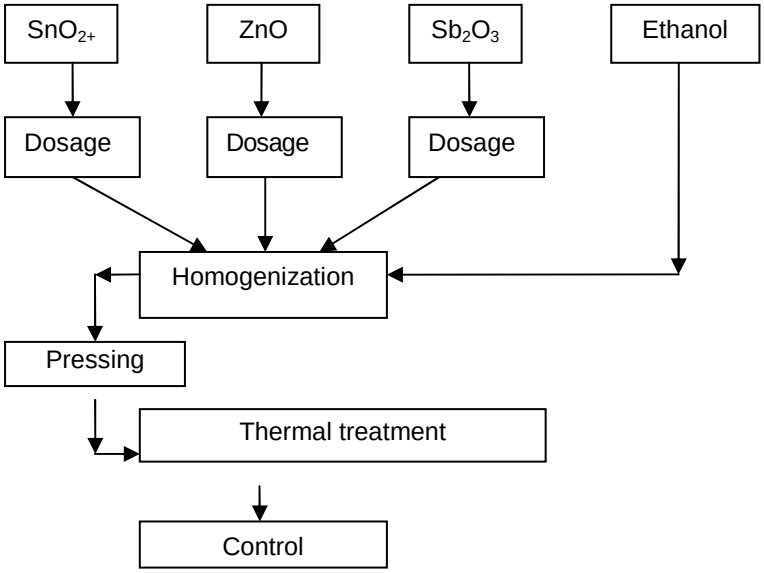

Figure 3. The schematic flux for obtaining the ceramics

The technological flux for obtaining the semiconductor ceramics with sensitive properties (figure 3) focused on reduction, as much as possible, of the possibilities for impurities to enter the system, on diminishing the loss of material, on a very good homogenization and milling of the components, in the view of obtaining an uniform microstructure following thermal treatment.

REFERENCES

1. Kim Hye-Kyung, S.D. Sathaye, Y.K. Hwang, S.H. Jhung, J-S. Hwang, S.H. Kwon, S-E. Park, J-S. Chang, *Bull.Korean Chem.Soc*., **2005**, *26* (11), 1881.
2. D.D. Vuong, G. Sakai, K. Shimanoe, N. Yamazoe, *Sensors and Actuators*, **2005**, *105*, 437.
3. G.G. Lee, L.S-J. Kang, *Sensors and actuators*, **2005**, *107*, 392.
4. Y. Shimizu, A. Jano, T. Hyodo, M. Egashira, *Sensors and Actuators*, **2005**, *108*, 56.
5. T.P. Hulser, H. Wiggers, A. Lorke, *Sensors and Actuators*, **2005**, *109*, 13.
6. Fan Jiwei, et al., *Journal of the European Ceramic Society*, **2010**, *30*, 545.
7. H.C. Wang, M.J. Yang, Y. Li, *Sensors and Actuators*, **2006**, *119*, 380.
8. W. Dang, H. Ping, D. Xiaowen, P. Qungyi, *Sensors and Actuators*, **2005**, *140*, 383.
9. M. Hayashi, T. Hyodo, Y. Shimitzu, M. Egashira, *Sensors and Actuators,* **2009**, *141*, 465.
10. A. Somăcescu, E. Andronescu, C. Somăcescu, *Rev. Rom. de Materiale*, **2003**, XXXIII (2), 85.
11. E.A. Guşă, I. Teoreanu, A. Petrescu, M. Ionescu, M. Bârlădeanu, *Rev. Rom. de Materiale*, **2009**, *39* (1), 57.
13. D.E. Dyshel, *Power Metallurgy and Metal Ceramics*, **2001**, *40* (5-6), 282.
14. M.A.L. Margionte, A.Z. Simoes, C.S. Riccardi, F.M. Filho, A. Ries, L. Perazolli, J.A. Varela, *Ceramics International*, **2006**, *32*, 713.
15. Li Laifeng, Pan Xiaoqing, *Chinese Journal of Materials Research*, **2000**, *14* (1), 42.
16. V. Geraldo, et al., *Materials Research*, **2003**, *6* (4), 451.